Iranian Journal of Numerical Analysis and Optimization
Vol. 16, No. 3, 2026, pp 1009–1030
https://doi.org/10.22067/ijnao.2026.93855.1660
https://ijnao.um.ac.ir/

Research Article

Barycentric rational interpolation method for fractional-order differential equation model of HIV infection of CD4$^+$T-cells

Kh. Divsar and R. Katani*

Abstract

In this work, we study HIV infection dynamics through fractional-order differential equations (FDEs), which have gained significant attention due to their ability to model complex biological processes with greater accuracy. The fractional-order models provide a more flexible framework by incorporating memory effects and hereditary properties, which are crucial in understanding the progression of HIV infection in CD4$^+$T-cells. This paper introduces a novel numerical method for solving the FDE model of HIV infection by transforming the FDE system into a system of weakly singular Volterra integral equations and applying a collocation method based on barycentric rational interpolation. A convergence analysis is given, and the estimated error is determined. This approach aims to enhance the accuracy and applicability of numerical solutions in modeling HIV dynamics. Numerical examples are provided to demonstrate the applicability and effectiveness of the proposed method.

*Corresponding author

Received 1 June 2025; revised 3 May 2026; accepted 9 May 2026

Khatoon Divsar
Faculty of sciences, Yasouj University, Yasouj - Iran. e-mail: divsark@gmail.com

Roghayeh Katani
Faculty of sciences, Yasouj University, Yasouj - Iran. e-mail: katani@yu.ac.ir

This article was suggested by the scientific committee of the 17th seminar on differential equation and dynamical system for publication in IJNAO, which was accepted after independent review

How to cite this article

Divsar, Kh. and Katani, R., Barycentric rational interpolation method for fractional-order differential equation model of HIV infection of CD4$^+$T-cells. *Iran. J. Numer. Anal. Optim.*, 2026; 16(3): 1009-1030. https://doi.org/10.22067/ijnao.2026.93855.1660

AMS subject classifications (2020): Primary 65R20; Secondary , 45D05.

Keywords: Model of HIV infection of CD4$^+$T-cells; Fractional differential equation; Barycentric rational interpolation; Error analysis.

1 Introduction

The mathematical modeling of HIV infection dynamics has long been a critical tool for understanding the complex interplay between viral replication and the immune response. Among the key components of such models, the interaction of HIV with CD4$^+$T-cells (a primary target of the virus) has been extensively studied using systems of differential equations. Perelson, Kirschner, and Boer [27] proposed an ordinary differential equation (ODE) model with four components: uninfected healthy CD4$^+$T-cells, latently infected CD4$^+$T-cells, actively infected CD4$^+$T-cells, and free virus. Other authors have proposed many models that take this model as their inspiration. Culshaw and Ruan [9] simplified the model of Perelson et al. into one consisting of only three components— healthy CD4$^+$T-cells, infected CD4$^+$T-cells, and free virus —and they introduced a discrete time delay to the model.

These integer-order models have provided invaluable insights, but they are inherently local, meaning the rate of change of the system's state depends only on its current state. Recent studies have shown that classical integer-order HIV models, while successful in capturing short-term viral dynamics, are often limited in representing the long-term and history-dependent processes inherent in immunological systems. Traditional ODE models assume that the rate of change of viral and cellular populations depends only on their present state, thereby neglecting the influence of past biological activity on current infection progression [11, 28]. However, clinical observations indicate that HIV dynamics exhibit long-term memory effects such as delayed immune activation, progressive loss of CD4$^+$T-cell regenerative capacity, and persistent viral reservoirs that continue to influence the system over time. Fractional-order models, incorporating derivatives of noninteger order, provide a mathematically rigorous framework for representing such hereditary and nonlocal effects through their intrinsic memory kernels [16, 7]. This makes fractional modeling particularly suitable for chronic viral infections like HIV, where immune responses and viral replication are governed not only by current viral load but also by accumulated infection history.

Recent advances in fractional calculus have motivated the use of fractional-order differential equations (FDEs) to better capture memory effects and nonlocal dynamics inherent in biological systems, offering a more nuanced representation of HIV pathogenesis. These models offer a

more realistic representation of HIV infection dynamics by accounting for the complex interactions and memory effects in biological systems [5]. The ability of fractional differential equations to accurately capture the dynamics of HIV infection in $CD4^+$T-cells is highlighted in previous works. For example, Sokhanvar and Askari-Hemmat [30] proposed a Galerkin method based on Legendre multi-wavelet functions to obtain approximate solutions of a fractional model for HIV infection of $CD4^+$T cells. In [8], a Laplace Adomian decomposition method was introduced for solving this model. Also, an Adams–Bashforth–Moulton method for the fractional model of HIV infection of $CD4^+$T-cells was presented in [19]. Whereas the methods mentioned above provide valuable tools for solving fractional HIV models, the development of efficient and high-order numerical schemes remains an active area of research. Recent literature has continued to explore novel approaches to handle the complexities of fractional systems. For instance, a Haar collocation method has been applied to a first-order model of HIV infection $CD4^+$T-Cells model in [3]. A quasi-linearization and Lagrangian method has been used for solving an integer order model of the HIV infection of $CD4^+$T-cells in [26]. This approach is based on the Lagrangian method by using the collocation points of transformed Hermite polynomials. Furthermore, the authors in [33] have proposed a numerical method based on novel Bessel polynomials for solving the fractional-order HIV-1 infection model of CD T-cells. This method considers the impact of antiviral drug treatment for solving a fractional-order HIV infection model, highlighting its utility as a fundamental computational tool. Alshammari et al. proposed an HIV model incorporating the impact of antiretroviral medication via the Caputo–Fabrizio derivative and presented a numerical study that investigates the complex dynamics of HIV infection in $CD4^+$T cells [2]. These recent contributions highlight the ongoing quest for numerical methods that combine computational efficiency with high precision for fractional-order biological models.

Despite these advances, a significant challenge persists: the nonlocal nature of fractional derivatives often leads to numerical methods that are computationally expensive or suffer from stability issues, especially when dealing with the weak singularities inherent in the kernel of the equivalent Volterra integral equation form. Many existing methods, including some of those cited, can be limited by low-order convergence, complex implementation, or a lack of a robust theoretical foundation for handling such singularities efficiently. This creates a clear gap for a high-order, computationally efficient, and numerically stable scheme specifically designed for systems of fractional differential equations with weak singular kernels.

In this paper, we consider the FDE model proposed by Dinga and Yea [10]. This model consists of three components and is actually a fractional version of the Culshaw and Ruan model [9]. We address the fractional-order HIV infection model of $CD4^+$T-cells by transforming the system of FDEs into a system of weakly singular Volterra integral equations (SWSVIEs). This reformulation not only mitigates the analytical complexities of fractional operators but also pro-

vides a robust framework for numerical approximation. In the following, we propose a novel collocation method based on barycentric rational interpolation to solve the resulting SWSVIEs. Our contribution is a tailored numerical scheme that directly addresses the gap of efficiently solving SWSVIEs arising from fractional biological models. The proposed method leverages the well-documented stability and high accuracy of barycentric rational interpolation, which is particularly adept at handling singular integrands without requiring specialized graded meshes, thus maintaining a simpler implementation profile than many competing high-order methods. This interpolation has emerged as a powerful tool in the numerical solution of integral equations, particularly Volterra integral equations. Huang et al. applied collocation methods based on barycentric rational interpolation to Volterra integro-differential equations with weakly singular kernels [35]. The authors in [22] combined discrete techniques on graded meshes with barycentric rational interpolation to address time-dependent partial integro-differential equations with weakly singular kernels. The method achieved second-order convergence in time. In [23], reducible quadrature rules were explored using barycentric rational interpolation, which do not require additional moment calculations. These rules demonstrated high-order convergence and extensive stability regions. Also, Li and Huang [21] developed a composite quadrature method for auto-convolution Volterra integral equations, based on linear barycentric rational interpolation. By leveraging this approach, we develop an efficient algorithm that avoids the stiffness often encountered in traditional discretization methods for FDEs. Numerical experiments demonstrate the method's precision, convergence, and applicability to real-world scenarios, underscoring its potential as a reliable tool for simulating fractional-order biomedical systems.

This paper is organized as follows: Section 2 introduces the fractional HIV infection model and its transformation to a Volterra integral system. Section 3 provides details of the barycentric rational collocation technique. The convergence analysis and the corresponding order of convergence are established in Section 4. Furthermore, Section 5 introduces an error estimator, which is particularly useful for problems where an exact solution is unknown. Numerical results demonstrating the efficacy of the proposed method are presented in Section 6, followed by a discussion and biological interpretation in Section 7. Finally, concluding remarks and future research directions are discussed in Section 8.

2 Fractional differential model

We first recall from [28] the main definitions and outcomes of fractional calculus that will be used in the following.

Definition 1. The operator J_a^α of order $\alpha \geq 0$ of the function y is given by

$$J_a^\alpha y(t) = \begin{cases} \frac{1}{\Gamma(\alpha)} \int_a^t \frac{y(s)}{(t-s)^{1-\alpha}} ds, & \alpha > 0, \\ y(t), & \alpha = 0, \end{cases}$$

and called the Riemann–Liouville fractional integral operator.

Definition 2. The Caputo fractional derivative of order $n-1 < \alpha \leq n$ $(n \in \mathbb{N})$ for $y \in AC^n([a,T])$ is defined as

$${}_a^C D_t^\alpha y(t) = \begin{cases} \frac{1}{\Gamma(n-\alpha)} \int_a^t \frac{y^{(n)}(s)}{(t-s)^{1+\alpha-n}} ds, & n-1 < \alpha < n, \\ y^{(n)}(t), & \alpha = n. \end{cases}$$

Proposition 1. TPodlubny) Based on the previous definitions, we have

$${}_0^C D_t^\alpha (J_0^\alpha y(t)) = y(t), \quad J_0^\alpha \left({}_0^C D_t^\alpha y(t)\right) = y(t) - \sum_{i=0}^{n-1} \frac{t^i}{i!} y^i(0). \tag{1}$$

2.1 Conversion to an SWSVIE

Consider FDE model proposed by Dinga and Yea [10] with some initial conditions in the form

$$\begin{aligned} {}_0^C D_t^\alpha T(t) &= s - \mu_T T(t) + rT(t)\left(1 - \frac{T(t)+I(t)}{T_{\max}}\right) - \kappa_1 V(t) T(t), \\ {}_0^C D_t^\alpha I(t) &= \kappa_1' V(t) T(t) - \mu_I I(t), \\ {}_0^C D_t^\alpha V(t) &= N\mu_b I(t) - \kappa_1 V(t) T(t) - \mu_V V(t), \quad 0 \leq t \leq R < \infty, \\ T(0) &= T_0, \quad I(0) = I_0, \quad V(0) = V_0, \end{aligned} \tag{2}$$

where $T(t)$ represents the concentration of healthy CD4$^+$T-cells at time t, $I(t)$ represents the concentration of infected CD4$^+$T-cells, and $V(t)$ the concentration of free HIV at time t. Here, $0.5 < \alpha \leq 1$ is restricted. When $0 < \alpha \leq 0.5$, we do not think fractional derivatives can approximately describe the rate of change in number [10].

Following, note that s is the source of CD4$^+$T-cells from precursors, μ_T is the natural death rate of CD4$^+$T-cells ($\mu_T T_{\max} > s$, see [27, p. 85]), r is their growth rate (thus, $r > \mu_T$ in general), and $T_{\max}$ is their carrying capacity. The parameter κ_1, represents the rate of infection of T-cells with free virus. κ_1' is the rate at which infected cells become actively infected. μ_I is a blanket death term for infected cells, to reflect the assumption that we do not initially know whether the cells die naturally or by bursting. In addition, μ_b is the lytic death rate for infected cells. Since

N viral particles are released by each lysing cell, this term is multiplied by the parameter N to represent the source for free virus (assuming a one-time initial infection). Finally, μ_V is the loss rate of virus.

The initial conditions for infection by free virus are $T(0) = T_0, I(0) = 0, V(0) = V_0$, where

$$T_0 = \frac{r - \mu_T + \left[(r-\mu_T)^2 + 4rsT_{\max}^{-1}\right]^{1/2}}{2rT_{\max}^{-1}}.$$

The parameter values given in Table 1.

By applying the operator J_0^α to both sides of (2) and by using Proposition 1, we obtain the equivalent system

$$\begin{aligned}
T(t) &= T_0 + \frac{1}{\Gamma(\alpha)} \int_0^t (t-\tau)^{\alpha-1} \left(s - \mu_T T + rT(1 - \frac{T+I}{T_{\max}}) - \kappa_1 VT \right) d\tau, \\
I(t) &= I_0 + \frac{1}{\Gamma(\alpha)} \int_0^t (t-\tau)^{\alpha-1} \left(\kappa_1' VT - \mu_I I \right) d\tau, \\
V(t) &= V_0 + \frac{1}{\Gamma(\alpha)} \int_0^t (t-\tau)^{\alpha-1} \left(N\mu_b I - \kappa_1 VT - \mu_V V \right) d\tau.
\end{aligned} \tag{3}$$

Consider

$$\begin{aligned}
K_1(t,T,I,V) &:= s - \mu_T T + rT\left(1 - \frac{T+I}{T_{\max}}\right) - \kappa_1 VT, \\
K_2(t,T,I,V) &:= \kappa_1' VT - \mu_I I, \\
K_3(t,T,I,V) &:= N\mu_b I - \kappa_1 VT - \mu_V V.
\end{aligned}$$

Therefore, we can obtain the matrix form

$$\mathbf{f}(t) = \mathbf{g} + \int_0^t \mathbf{p}(t,\tau)\mathbf{K}(\tau,\mathbf{f})d\tau,$$

where

$$\begin{aligned}
\mathbf{f} &= (T,I,V)^\top, & \mathbf{p}(t,\tau) &= \left((t-\tau)^{\alpha-1}, (t-\tau)^{\alpha-1}, (t-\tau)^{\alpha-1}\right)^\top, \\
\mathbf{g} &= (T_0, I_0, V_0)^\top, & \mathbf{K}(\tau,\mathbf{f}) &= \frac{1}{\Gamma(\alpha)} \left(K_1(\tau,\mathbf{f}^\top), K_2(\tau,\mathbf{f}^\top), K_3(\tau,\mathbf{f}^\top) \right).
\end{aligned}$$

Table 1: Parameters and variables [10]

		Values
T	Uninfected CD4$^+$T-cell population size	$T_0 = 1000\ mm^{-3}$
I	Infected CD4$^+$T-cell density	$I_0 = 0$
V	Initial density of HIV RNA	$V_0 = 10^{-3}\ mm^{-3}$
μ_T	Natural death rate of CD4$^+$T-cells	$0.02\ day^{-1}$
μ_I	Blanket death rate of infected CD4$^+$T-cells	$0.26\ day^{-1}$
μ_b	Lytic death rate for infected cells	$0.24\ day^{-1}$
μ_v	Death rate of free virus	$2.4\ day^{-1}$
κ_1	Rate CD4$^+$T-cells become infected with virus	$2.4 \times 10^{-5}\ mm^3\ day^{-1}$
κ_1'	Rate infected cells become active	$2 \times 10^{-5}\ mm^3\ day^{-1}$
r	Growth rate of CD4$^+$T-cells population	$0.03\ day^{-1}$
N	Number of virions produced by infected CD4$^+$T-cells	Varies
$T_{\max}$	Maximal population level of CD4$^+$T-cells	$1500\ mm^{-3}$
s	Source term for uninfected CD4$^+$T-cells	$10\ day^{-1}\ mm^{-3}$
T_0	CD4$^+$ T-cells population for HIV-negative persons	$1000\ mm^{-3}$

3 Numerical method

Generally, the singularities of the kernel functions of the system (3) may cause a nonsmooth solution, and its derivative to be singular near the integral domain boundary. In these cases, by a smoothing transformation, we can recover the smooth property of the solution, (for more details, see [14, 17, 20]). In the following, we assume that the solutions of the system (3) are smooth.

Given $n+1$ strictly ordered interpolation points $t_0 < t_1 < \cdots < t_n$ and the associated values $y_0, y_1, \ldots, y_n$, for each $i = 0, 1, \ldots, n-d$, $0 \le d \le n$, let p_i be the polynomials of degree at most d which interpolate the $d+1$ data pairs $\{(t_i, y_i), (t_{i+1}, y_{i+1}), \ldots, (t_{i+d}, y_{i+d})\}$ of $y(t)$, $t \in [0, R]$, with $y_k = y(t_k)$, $k = 0, 1, \ldots, n$. Then the Floater and Hormann rational interpolation function [12] is

$$r(t) = \frac{\sum_{i=0}^{n-d} \lambda_i(t) p_i(t)}{\sum_{i=0}^{n-d} \lambda_i(t)}, \qquad \lambda_i(t) = \frac{(-1)^i}{(t-t_i)(t-t_{i+1})\cdots(t-t_{i+d})}, \tag{4}$$

where $\lambda_i(t)$ are the original rational interpolation weights and d is the rational interpolation parameter.

Lemma 1. [12] For any $d \in \{0, 1, \ldots, n\}$, the rational interpolation $r(t)$ has no poles.

Lemma 2. [12] For any $d \in \{1, \ldots, n\}$ and $y \in C^{d+2}[0,1]$, then the error bound can be obtained as

$$\| y - r \| \leq \begin{cases} h^{d+1} \frac{\|u^{(d+2)}\|}{d+2}, & \text{if } n-d \text{ is odd,} \\ h^{d+1} \left(\frac{\|u^{(d+2)}\|}{d+2} + \frac{\|u^{(d+1)}\|}{d+1} \right), & \text{if } n-d \text{ is even,} \end{cases}$$

with $h = \max\limits_{0 \leq i \leq n-1} (x_{i+1} - x_i)$.

Furthermore, for equidistant nodes, the modified barycentric Floater–Hormann weight functions are introduced as $\alpha_i = (-1)^{i-d} \sum\limits_{k \in J_i} \begin{pmatrix} d \\ i-k \end{pmatrix}$ where $J_i = \{k \in I : i-d \leq k \leq i, I = \{0, 1, \ldots, n\}\}$ is an index set. As shown in [12], (4) can be rewritten as

$$r_n[y](t) = \sum_{i=0}^{n} \phi_i(t) y_i, \quad \phi_i(t) = (\frac{\alpha_i}{t - t_i}) / (\sum_{k=0}^{n} \frac{\alpha_k}{t - t_k}), \tag{5}$$

where $\phi_i(t), i = 0, 1, \ldots, n$ are called barycentric rational interpolation basis functions, which satisfy the Lagrange property $\phi_i(t_k) = \delta_{ik}, k = 0, 1, \ldots, n$ with δ_{ik} being the Kronecker-delta functions. Consider $T(t_i) \approx T_i$, $I(t_i) \approx I_i$, $V(t_i) \approx V_i$, therefore the solution of system (3) may be approximated by the representation $K_l(t, T(t), I(t), V(t)) \approx r_n[K_l](t)$, for $l = 1, 2, 3$ and we will have

$$\begin{aligned} T_j &= T_0 + \frac{1}{\Gamma(\alpha)} \sum_{i=0}^{n} K_{1,i} \int_0^{t_j} (t_j - \tau)^{\alpha-1} \phi_i(\tau) d\tau, \\ I_j &= I_0 + \frac{1}{\Gamma(\alpha)} \sum_{i=0}^{n} K_{2,i} \int_0^{t_j} (t_j - \tau)^{\alpha-1} \phi_i(\tau) d\tau, \\ V_j &= V_0 + \frac{1}{\Gamma(\alpha)} \sum_{i=0}^{n} K_{3,i} \int_0^{t_j} (t_j - \tau)^{\alpha-1} \phi_i(\tau) d\tau, \qquad j = 1, 2, \ldots, n, \end{aligned} \tag{6}$$

where the collocation nodes t_j are the same as the interpolation nodes and $K_{l,i} := K_l(t_i, T_i, I_i, V_i)$, for $l = 1, 2, 3$.

The calculation of the above integral is crucial to achieve a highly accurate solution of (3); by using variable transformation $\tau = \frac{t_j}{2} s + \frac{t_j}{2}$ we obtain

$$\int_0^{t_j} (t_j - \tau)^{\alpha-1} \phi_i(\tau) d\tau = (\frac{t_j}{2})^{\alpha} \int_{-1}^{1} (1-s)^{\alpha-1} \phi_i(\frac{t_j}{2} s + \frac{t_j}{2}) ds,$$

then we can use the Gauss–Jacobi quadrature rule with the weights ω_q and the corresponding nods σ_q to approximate them. Then, a discrete system can be obtained as

$$
\begin{aligned}
T_j &= T_0 + \frac{1}{\Gamma(\alpha)} \sum_{i=0}^{n} K_{1,i} \sum_{q=1}^{N} \omega_q (1-\sigma_q)^{\alpha-1} \phi_i(\frac{t_j}{2}\sigma_q + \frac{t_j}{2}),\\
I_j &= I_0 + \frac{1}{\Gamma(\alpha)} \sum_{i=0}^{n} K_{2,i} \sum_{q=1}^{N} \omega_q (1-\sigma_q)^{\alpha-1} \phi_i(\frac{t_j}{2}\sigma_q + \frac{t_j}{2}),\\
V_j &= V_0 + \frac{1}{\Gamma(\alpha)} \sum_{i=0}^{n} K_{3,i} \sum_{q=1}^{N} \omega_q (1-\sigma_q)^{\alpha-1} \phi_i(\frac{t_j}{2}\sigma_q + \frac{t_j}{2}), \qquad j = 1, 2, \ldots, n.
\end{aligned} \tag{7}
$$

The above system can be rewritten in matrix form

$$
\mathbf{f}_j = \mathbf{g} + \sum_{i=0}^{n} \mathbf{K}_i \sum_{q=1}^{N} \omega_q \mathbf{p}(t_j, \sigma_q) \phi_i(\frac{t_j}{2}\sigma_q + \frac{t_j}{2}),
$$

where

$$
\begin{aligned}
&\mathbf{f}_j = (T_j, I_j, V_j)^\top, && \mathbf{g} = (T_0, I_0, V_0)^\top,\\
&\mathbf{p}(t_j, \sigma_q) = \left((t_j-\sigma_q)^{\alpha-1}, (t_j-\sigma_q)^{\alpha-1}, (t_j-\sigma_q)^{\alpha-1}\right)^\top,\\
&\mathbf{K}_i = \frac{1}{\Gamma(\alpha)} \left(K_1(t_i, T_i, I_i, V_i), K_2(t_i, T_i, I_i, V_i), K_3(t_i, T_i, I_i, V_i)\right).
\end{aligned}
$$

Finally, the obtained system can be solved by Newton's iterative method, therefore we can obtain the values of the unknown functions at the mesh points by solving system (7) for $j = 1, 2, \ldots, n$.

4 Convergence analysis

Theorem 1. Let the kernels K_l $(l = 1, 2, 3)$ satisfy a Lipschitz condition with respect to all variables except for the first. Then the solution of the discrete system (6) is convergent to the solution of the system (3), and the order of convergence is $O(h^{\alpha+d+1})$.

Proof. Let $\mathbf{e}_j := \mathbf{f} - \mathbf{f}_j$, without loss of generality, suppose that $\| \mathbf{e}_j \|_\infty = \max_j |T(t_j) - T_j|$. Therefore by subtracting (6) from (3), we have

$$
\begin{aligned}
T(t_j) - T_j =& \frac{1}{\Gamma(\alpha)} \int_0^{t_j} (t_j-\tau)^{\alpha-1} K_1(\tau, T, I, V) d\tau\\
&- \frac{1}{\Gamma(\alpha)} \sum_{i=0}^{n} K_{1,i} \int_0^{t_j} (t_j-\tau)^{\alpha-1} \phi_i(\tau) d\tau\\
=& \frac{1}{\Gamma(\alpha)} \int_0^{t_j} (t_j-\tau)^{\alpha-1} \Big[K_1(\tau, T, I, V)
\end{aligned}
$$

$$-\sum_{i=0}^{n} K_1(t_i, T(t_i), I(t_i), V(t_i))\phi_i(\tau)\Big] d\tau$$
$$+\frac{1}{\Gamma(\alpha)}\sum_{i=0}^{n}[K_1(t_i, T(t_i), I(t_i), V(t_i))$$
$$-K_1(t_i, T_i, I_i, V_i)]\int_0^{t_j}(t_j-\tau)^{\alpha-1}\phi_i(\tau)d\tau. \quad (8)$$

To guarantee the existence and uniqueness of the solution, we assume that the kernels $K_l(l = 1, 2, 3)$ satisfy a Lipschitz condition with respect to all variables except for the first [18, 25]. Applying Lemma 2 and using Lipschitz condition leads to

$$\| \mathbf{e}_j \|_\infty \leq \frac{h^{d+1}}{(d+2)\Gamma(\alpha)} \| \frac{\partial^{d+2}K}{\partial t^{d+2}} \| \int_0^{t_j}(t_j-\tau)^{\alpha-1}d\tau$$
$$+\frac{L}{\Gamma(\alpha)}\sum_{i=0}^{n}\| \mathbf{f}(t_j)-\mathbf{f}_j \| \int_0^{t_j}(t_j-\tau)^{\alpha-1}\phi_i(\tau)d\tau,$$

where $n-d$ is odd and L is the Lipschitz constant. Equivalently,

$$\| \mathbf{e}_j \|_\infty \leq \frac{h^{\alpha+d+1}j^\alpha}{\alpha(d+2)\Gamma(\alpha)} \| \frac{\partial^{d+2}K}{\partial t^{d+2}} \|$$
$$+\frac{Lj^\alpha h^\alpha}{2\Gamma(\alpha)}\sum_{i=0}^{n}\| \mathbf{e}_i \| \int_{-1}^{1}(1-s)^{\alpha-1}\phi_i(\frac{t_j}{2}s+\frac{t_j}{2})ds$$
$$\leq C_1 h^{\alpha+d+1} + C_2 h^\alpha \sum_{i=0}^{n}\| \mathbf{e}_i \|,$$

where C_1, C_2 are constants. Similarly, for the case where $n-d$ is even, we can obtain

$$\| \mathbf{e}_j \|_\infty \leq \frac{h^{d+1}j^\alpha}{\alpha\Gamma(\alpha)}\left(\frac{1}{d+2}\| \frac{\partial^{d+2}K}{\partial t^{d+2}} \| + \frac{1}{d+1}\| \frac{\partial^{d+1}K}{\partial t^{d+1}} \|\right)$$
$$+\frac{Lj^\alpha h^\alpha}{2\Gamma(\alpha)}\sum_{i=0}^{n}\| \mathbf{e}_i \| \int_{-1}^{1}(1-s)^{\alpha-1}\phi_i(\frac{t_j}{2}s+\frac{t_j}{2})ds$$
$$\leq C_1 h^{\alpha+d+1} + C_2 h^\alpha \sum_{i=0}^{n}\| \mathbf{e}_i \| .$$

Now, consider $\| \mathbf{e} \|_\infty = \max_{j=1,2,\ldots,n} \| \mathbf{e}_j \|_\infty = \| \mathbf{e}_n \|_\infty$. Then we will have

$$\| \mathbf{e}_n \|_\infty \leq \frac{C_1}{1-C_2h^\alpha}h^{\alpha+d+1} + \frac{C_2}{1-C_2h^\alpha}h^\alpha \sum_{i=0}^{n-1}\| \mathbf{e}_i \|,$$

and using the Grönwall's inequality (see [24]), yields

$$\| \mathbf{e}_n \|_\infty \leq \frac{C_1}{1 - C_2 h^\alpha} h^{\alpha+d+1} \exp\left(\frac{C_2}{1 - C_2 h^\alpha} t_n\right).$$

Hence $\| \mathbf{e}_n \|_\infty \to 0$ as $h \to 0$ and the order of convergence is $O(h^{\alpha+d+1})$ which completes the proof. □

5 Error estimation

In this section, we obtain the error estimation (see [1, 31]) for HIV model (2) utilizing barycentric rational interpolation method. The residual functions $R_{1,n}(t)$, $R_{2,n}(t)$, and $R_{3,n}(t)$ are

$$\begin{aligned}
R_{1,n}(t) &= {}_0^C D_t^\alpha T_n(t) - s + \mu_T T_n(t) - r T_n(t)\left(1 - \frac{T_n(t) + I_n(t)}{T_{\max}}\right) \\
&\quad + \kappa_1 V_n(t) T_n(t), \\
R_{2,n}(t) &= {}_0^C D_t^\alpha I_n(t) - \kappa_1' V_n(t) T_n(t) + \mu_I I_n(t), \\
R_{3,n}(t) &= {}_0^C D_t^\alpha V_n(t) - N\mu_b I_n(t) - \kappa_1 V_n(t) T_n(t) + \mu_V V_n(t), \quad 0 \leq t \leq R < \infty.
\end{aligned} \tag{9}$$

Let the error functions be

$$\begin{aligned}
e_{1,n}(t) &= T(t) - T_n(t), \\
e_{2,n}(t) &= I(t) - I_n(t), \\
e_{3,n}(t) &= V(t) - V_n(t),
\end{aligned} \tag{10}$$

where $T(t)$, $I(t)$, and $V(t)$ are exact solutions. Subtracting (9) from (2) leads to

$$\begin{aligned}
{}_0^C D_t^\alpha (T(t) - T_n(t)) =& -\mu_T (T(t) - T_n(t)) + r(T(t) - T_n(t)) \\
& - \frac{r}{T_{\max}} \left[T^2(t) - T_n^2(t) + T(t)I(t) - T_n(t)I_n(t)\right] \\
& - \kappa_1 (V(t)T(t) - V_n(t)T_n(t)) - R_{1,n}(t), \\
{}_0^C D_t^\alpha (I(t) - I_n(t)) =& \kappa_1' (V(t)T(t) - V_n(t)T_n(t)) - \mu_I (I(t) - I_n(t)) - R_{2,n}(t), \\
{}_0^C D_t^\alpha (V(t) - V_n(t)) =& N\mu_b (I(t) - I_n(t)) - \kappa_1 (V(t)T(t) - V_n(t)T_n(t)) \\
& - \mu_V (V(t) - V_n(t)) - R_{3,n}(t),
\end{aligned} \tag{11}$$

By adding and subtracting some terms and using relations (10), we have

$$
\begin{aligned}
{}_0^C D_t^\alpha e_{1,n}(t) =& -\mu_T e_{1,n}(t) + r e_{1,n}(t) - \frac{r}{T_{\max}}\left[T^2(t) \pm 2T(t)T_n(t) \pm T_n^2(t)\right.\\
&\left. -T_n^2(t) + T(t)I(t) - T_n(t)I_n(t) \pm I(t)T_n(t)\right]\\
&-\kappa_1\left[V(t)T(t) - V_n(t)T_n(t) \pm V(t)T_n(t)\right] - R_{1,n}(t),\\
{}_0^C D_t^\alpha e_{2,n}(t) =& \kappa_1'\left[V(t)T(t) - V_n(t)T_n(t) \pm V(t)T_n(t)\right] - \mu_I e_{2,n}(t) - R_{2,n}(t),\\
{}_0^C D_t^\alpha e_{3,n}(t) =& N\mu_b e_{2,n}(t) - \kappa_1\left[V(t)T(t) - V_n(t)T_n(t) \pm V(t)T_n(t)\right]\\
&-\mu_V e_{3,n}(t) - R_{3,n}(t).
\end{aligned} \tag{12}
$$

Then we obtain

$$
\begin{aligned}
{}_0^C D_t^\alpha e_{1,n}(t) =& -\mu_T e_{1,n}(t) + r e_{1,n}(t) - \frac{r}{T_{\max}}\left[e_{1,n}^2(t) + 2T_n e_{1,n}(t) + T_n e_{2,n}(t)\right.\\
&\left. + I e_{1,n}(t)\right] - \kappa_1 V e_{1,n}(t) - \kappa_1 T_n e_{3,n}(t) - R_{1,n}(t),\\
{}_0^C D_t^\alpha e_{2,n}(t) =& \kappa_1' V e_{1,n}(t) + \kappa_1' T_n e_{3,n}(t) - \mu_I e_{2,n}(t) - R_{2,n}(t),\\
{}_0^C D_t^\alpha e_{3,n}(t) =& N\mu_b e_{2,n}(t) - \kappa_1 V e_{1,n}(t) - \kappa_1 T_n e_{3,n}(t) - \mu_V e_{3,n}(t) - R_{3,n}(t).
\end{aligned} \tag{13}
$$

The initial conditions for the approximate solution of the HIV model are $T_n(0) = T_0$, $I_n(0) = I_0$, and $V_n(0) = V_0$. Therefore the initial values for system (13) will be $e_{1,n}(0) = e_{2,n}(0) = e_{3,n}(0) = 0$.

In the following, we estimate $e_{1,n}(t)$ $e_{2,n}(t)$ and $e_{3,n}(t)$ by using proposed barycentric interpolation method (Section 3). To accomplish this, we apply the operator J_0^α to both sides of (13); then we have

$$
\begin{aligned}
e_{1,n}(t) &= e_{1,n}(0) + \frac{1}{\Gamma(\alpha)}\int_0^t (t-\tau)^{\alpha-1} k_1(\tau, e_{1,n}, e_{2,n}, e_{3,n})d\tau,\\
e_{2,n}(t) &= e_{2,n}(0) + \frac{1}{\Gamma(\alpha)}\int_0^t (t-\tau)^{\alpha-1} k_2(\tau, e_{1,n}, e_{2,n}, e_{3,n})d\tau,\\
e_{3,n}(t) &= e_{3,n}(0) + \frac{1}{\Gamma(\alpha)}\int_0^t (t-\tau)^{\alpha-1} k_3(\tau, e_{1,n}, e_{2,n}, e_{3,n})d\tau,
\end{aligned}
$$

where

$$
\begin{aligned}
k_1(t, e_{1,n}, e_{2,n}, e_{3,n}) =& (r-\mu_T)e_{1,n}(t) - \frac{r}{T_{\max}}\left[e_{1,n}^2(t) + 2T_n e_{1,n}(t) + T_n e_{2,n}(t)\right.\\
&\left. + I e_{1,n}(t)\right] - \kappa_1 V e_{1,n}(t) - \kappa_1 T_n e_{3,n}(t) - R_{1,n}(t),\\
k_2(t, e_{1,n}, e_{2,n}, e_{3,n}) =& \kappa_1' V e_{1,n}(t) + \kappa_1' T_n e_{3,n}(t) - \mu_I e_{2,n}(t) - R_{2,n}(t),
\end{aligned}
$$

$$k_3(t, e_{1,n}, e_{2,n}, e_{3,n}) = N\mu_b e_{2,n}(t) - \kappa_1 V e_{1,n}(t) - \kappa_1 T_n e_{3,n}(t) - \mu_V e_{3,n}(t) - R_{3,n}(t).$$

In the same manner as described in section 3, we consider $e_{1,n}(t_i) \approx e^i_{1,n}$, $e_{2,n}(t_i) \approx e^i_{2,n}$, $e_{3,n}(t_i) \approx e^i_{3,n}$ and $k_l(t, e_{1,n}, e_{2,n}, e_{3,n}) \approx r_n[k_l](t) = \sum_{i=0}^{n} \phi_i(t) k_{l,i}$ where $k_{l,i} := k_l(t_i, e^i_{1,n}, e^i_{2,n}, e^i_{3,n}), l = 1, 2, 3$. Also, interpolate data pairs and barycentric rational interpolation basis function are similar to Section 3.

Finally, approximation the above integrals and using Gauss–Jacobi quadrature rule and solve the obtained system leads to estimate of the error functions $e_{1,n}(t)$, $e_{2,n}(t)$ and $e_{3,n}(t)$.

6 Numerical results

In this section, we conduct experimental tests to evaluate the convergence and measure the error of the proposed method. To do this, we carry out the numerical experiments employing the software "MATLAB R2016a" to find approximate solution. The order of the Gauss–Jacobi quadrature is chosen to balance the errors between interpolation and quadrature, for Gauss–Jacobi quadrature of order N we have

$$\left| \int_{-1}^{1} (1-s)^{\alpha-1} f(s) ds - \sum_{q=1}^{N} \omega_q f(\sigma_q) \right| \leq \frac{C}{N^{2m}} \|f^{(2m)}\|_\infty,$$

where m depends on the smoothness of f. Therefore, we should choose N such that

$$\text{Quadrature Error} \approx \text{Interpolation Error}.$$

This leads to the condition

$$\frac{C_{quad}}{N^{2m}} \approx C_{interp} h^{d+1}.$$

Therefore the optimal N satisfies

$$N \approx \left(\frac{C_{quad}}{C_{interp} h^{d+1}} \right)^{\frac{1}{2m}}.$$

First, we have to apply the method presented for model (2) with parameter values reported in Table 1. We consider the initial conditions $T(0) = 1000$, $I(0) = 0$ and $V(0) = 0.001$ in the time period of 100 days with the step length size $h = 0.1$.

The diagrams of the concentration of healthy CD4$^+$T cells (T), infected CD4$^+$T cells (I), and the concentration of HIV virus (V) in this time period for different values of α are shown

in Figures 1–3, respectively. The figures show that for the initial concentration $V = 10^{-3}mm^{-3}$ of HIV virus, after almost ten days, the concentration of healthy CD4$^+$T cells decreases rapidly, and the concentration of infected CD4$^+$T cells and HIV virus increase rapidly in the same proportion and after almost twenty days, the concentration of healthy cells becomes very low, while the concentration of infected cells and HIV virus remains high. Table 2 presents the

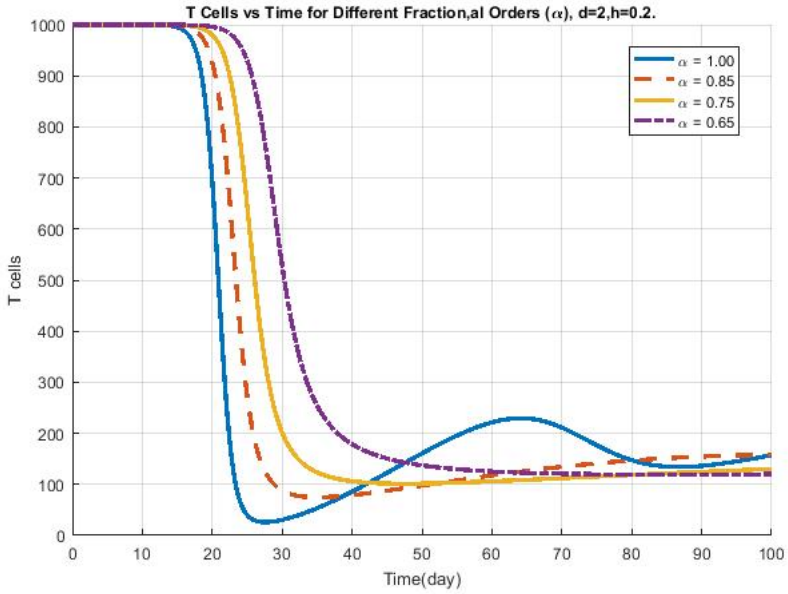

Figure 1: Rate of the concentration of healthy CD4$^+$T-cells ($T(t)$), for $d = 2$, $h = 0.2$.

estimated errors in the time period of 100 days with the step length size $h = 0.2$ at specific mesh points for $d = 2$. The results of this table show that the estimated errors for $\alpha = 0.65$ are significantly smaller, suggesting better stability for fractional orders.

To demonstrate the efficiency of the proposed method and provide comparisons with existing numerical approaches, consider [34]

$$\begin{aligned}
\frac{dT}{dt} &= 0.1 - 0.02 + T\left(1 - \frac{T+I}{1500}\right) - 0.0027VT,\\
\frac{dI}{dt} &= -0.0027VT - 0.3I,\\
\frac{dV}{dt} &= 10(0.3)I - 2.4V, \qquad\qquad 0 \le t \le 1,
\end{aligned} \tag{14}$$

with $T(0) = 0.1$, $I(0) = 0$ and $V(0) = 0.1$.

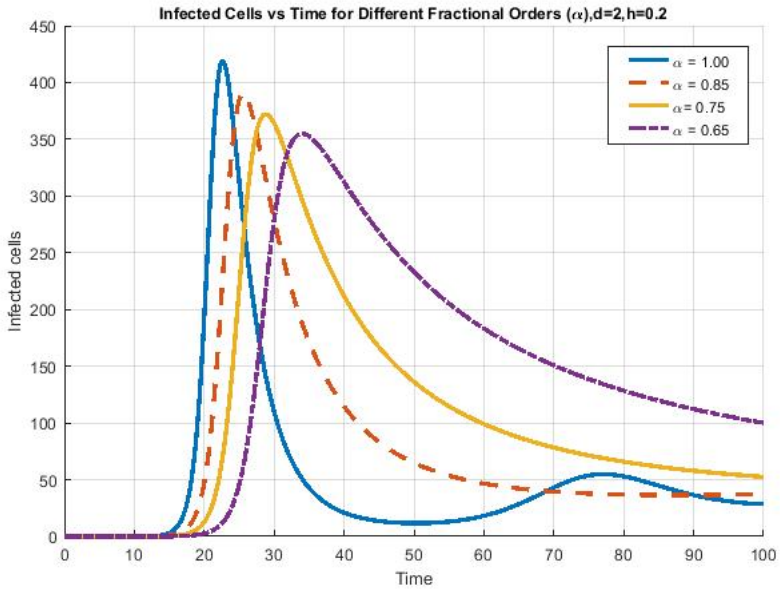

Figure 2: Rate of the concentration of infected CD4$^+$T-cells ($I(t)$)for $d = 2$, $h = 0.2$.

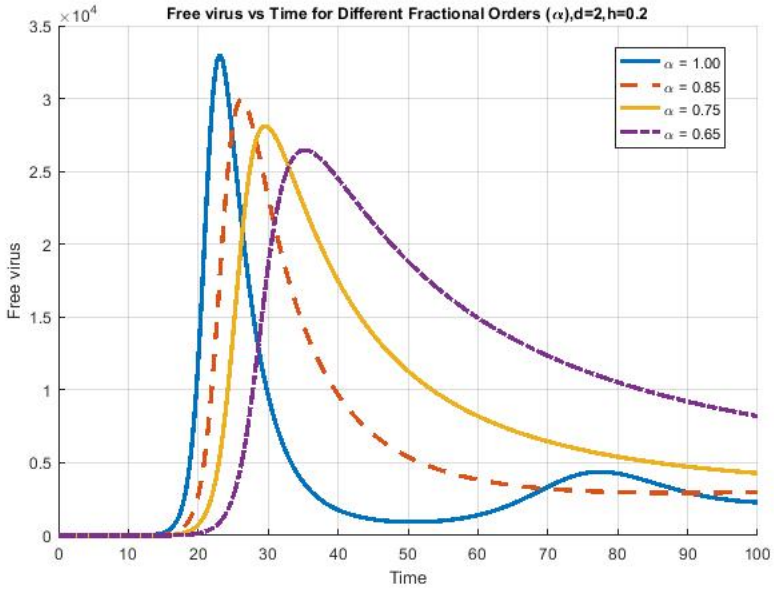

Figure 3: Rate of the concentration of free HIV virus ($V(t)$)for $d = 2$, $h = 0.2$.

Table 2: Estimated errors for parameter values of Table 1, $h = 0.2$, $d = 2$.

	$\alpha = 1$			$\alpha = 0.65$		
t	$e_{1,n}(t)$	$e_{2,n}(t)$	$e_{3,n}(t)$	$e_{1,n}(t)$	$e_{2,n}(t)$	$e_{3,n}(t)$
1	2.456e-08	5.712e-09	4.025e-09	0	0	0
10	3.104e-07	1.321e-08	1.182e-08	5.172e-11	4.065e-12	3.421e-12
20	6.461e-07	7.051e-08	4.315e-08	2.854e-10	8.421e-11	9.603e-11
40	2.603e-06	3.402e-07	9.124e-08	6.106e-10	2.207e-10	1.557e-11
60	1.781e-05	7.051e-05	4.315e-06	5.854e-09	9.217e-10	4.103e-10
80	6.821e-05	2.157e-04	1.052e-05	6.421e-08	3.165e-09	7.551e-10
100	1.004e-04	4.203e-04	5.167e-05	3.301e-07	6.781e-09	2.445e-09

In Tables 3–5, the values of the approximate solutions at some mesh points (with step length $h = 0.1$ and $d = 3$) are compared with the Runge–Kutta method, the Bessel collocation method [32], exponential Galerkin method [34], and Haar collocation algorithm [3].

The method's results in these tables are often the closest to the Runge–Kutta solution, sometimes even surpassing the other collocation methods. The close agreement with the Runge–Kutta method (the benchmark for integer-order ODEs) for the model from [34] confirms that our proposed method is numerically accurate and produces biologically plausible results.

Table 3: Comparison for uninfected cells $T(t)$.

t	Runge–Kutta	Bessel coll. [32]	Galerkin ($N = 5$) [34]	Haar coll. [3]	presented method
0.2	0.2087297222	0.2038616561	0.1982953765	0.2073431784	0.2087654367
0.4	0.4059409955	0.3803309335	0.4183153468	0.3930921357	0.4058215441
0.6	0.7635801781	0.6954623767	0.7603331972	0.6453087042	0.7634567891
0.8	1.4119574363	1.2759624442	1.4077147917	1.3978540981	1.4076542124
1.0	2.5867778755	2.3832277428	2.5915947135	2.5709802316	2.5854678912

7 Discussion and biological interpretation

The numerical simulations presented in this work provide insights into the progression of HIV infection and demonstrate the capability of the proposed numerical scheme to accurately capture the key biological characteristics of viral dynamics. The dynamics depicted in Figures 1–3 for the

Table 4: Comparison for infected $I(t)$.

t	Runge–Kutta	Bessel coll. [32]	Galerkin ($N = 5$) [34]	Haar coll. [3]	presented method
0.2	0.0000060315	0.0000062478	0.0000059641	0.0000070416	0.0000071256
0.4	0.0000131530	0.0000129355	0.0000131340	0.0000140251	0.0000134567
0.6	0.0000212106	0.0000203526	0.0000212682	0.0000230126	0.0000223456
0.8	0.0000301518	0.0000283730	0.0000301754	0.0000309231	0.0000312345
1.0	0.0000399942	0.0000369084	0.0000400377	0.0000403894	0.0000398122

Table 5: Comparison for free virus particles $V(t)$.

t	Runge–Kutta	Bessel coll. [32]	Galerkin ($N = 5$) [34]	Haar coll. [3]	presented method
0.2	0.0618798121	0.0618799185	0.0618799035	0.0617912741	0.0618797124
0.4	0.0382948730	0.0382949349	0.0382947890	0.0380026874	0.0382947891
0.6	0.0237045402	0.0237043186	0.0237046061	0.0236011879	0.0237041237
0.8	0.0146803506	0.0146795698	0.0146803810	0.0139672890	0.0146808541
1.0	0.0091008270	0.0090993030	0.0091008486	0.0089053621	0.00910084567

model (2) with the parameters from Table 1 recapitulate the well-established clinical progression of untreated HIV infection. The simulation can be interpreted as a representation of two key phases:

- The Acute Infection Phase (Days 0-10): The initial conditions, particularly the low viral load ($V(0) = 0.001$), simulate the moment of infection. The subsequent rapid decline in healthy CD4$^+$T-cells ($T(t)$) and the simultaneous rapid increase in both infected cells ($I(t)$) and free virus ($V(t)$) are hallmarks of the acute HIV syndrome. Biologically, this represents the uncontrolled replication and dissemination of the virus following its entry into the host. The virus specifically targets and hijacks the machinery of CD4$^+$T-cells. The immune activation leads to the observed sharp drop in $T(t)$, while the rise in $I(t)$ and $V(t)$ directly reflects the successful establishment and spread of the infection within the host.

- Transition to the Chronic Phase (After $\sim$ 20 days): The simulation shows the system reaching a new, pathological equilibrium where the concentration of healthy CD4$^+$T-cells remains critically low, while the populations of infected cells and free virus persist at high

levels. This state models the transition to the chronic phase of HIV infection. In a clinical setting, this corresponds to a patient with a high viral load and a low CD4 count, leaving them severely immunocompromised and vulnerable to opportunistic infections. The model's ability to capture this set-point is crucial, as the level at which this equilibrium is established is a strong predictor of the rate of disease progression to AIDS (The acute and chronic phases of HIV infection are discussed in [15], while [6] specifically addresses the establishment of a viral set-point during the asymptomatic stage and the critically low CD4 count characteristic of chronic infection).

An important contribution of the present study is the incorporation and analysis of fractional-order dynamics. The results demonstrate that solutions corresponding to fractional orders (e.g., $\alpha = 0.65$) display significantly improved numerical stability and lower estimation errors compared with the classical integer-order case (consistent with [4, 29] showing that fractional models are more biologically plausible for primary HIV infection). From a biological perspective, this observation suggests that fractional operators may better represent the intrinsic memory and hereditary properties of HIV infection, where the current state of the immune system is influenced by the history of viral–immune interactions. Such interpretations are compatible with experimental evidence indicating that viral replication, cell activation, and immune response processes involve delays and cumulative biological effects that cannot always be represented adequately by first-order derivative models. By capturing these nonlocal effects, the fractional formulation may be considered closer to the real underlying biological mechanisms, improving the descriptive and predictive power of mathematical models in immunology.

Furthermore, comparisons with existing numerical schemes, including Runge–Kutta methods, the Bessel collocation method, exponential Galerkin approaches, and Haar wavelet-based algorithms, indicate that the proposed method achieves superior computational performance in terms of accuracy and error control.

In general, the findings of this study highlight that the proposed numerical method advances current computational tools for HIV modeling by improving solution quality and enabling the study of biological memory effects. These advantages can be valuable in future investigations of therapeutic strategies, viral mutation dynamics, immune system degradation, and long-term patient response modeling.

8 Conclusion

This paper proposed a numerical method for solving a model of HIV infection of $CD4^+$T-cells. We considered the model as a fractional differential equations system and converted it to an

equivalent SWSVIEs (system of weakly singular Volterra integral equations). The obtained system was solved by a collocation method based on barycentric rational interpolation. We showed the numerical results for different values of α. The proposed method is convergent with high accuracy, simple, and can be applied to solve other cases of fractional differential equations.

The parameter d which controls the degree of the local polynomial interpolation used in the Floater–Hormann family of barycentric rational interpolations plays a crucial role in both the performance and numerical stability of the method. While higher d can improve theoretical accuracy for smooth functions, it also increases the risk of oscillations (a phenomenon akin to the Runge effect).

Although one cannot prescribe a universal optimal d, but for equidistant nodes, larger d generally improves stability in the first form [13]. Also, the numerical results show that both error and cost depend significantly on d. Future work could include a systematic sensitivity analysis or a heuristic for choosing d based on node distribution and desired accuracy.

Funding

This research received no external funding.

Conflicts of Interest

The authors declare no conflicts of interest.

References

[1] Abbasi, Z., Izadi, M. and Hosseini, M.M. *A highly accurate matrix method for solving a class of strongly nonlinear BVP arising in modeling of human shape corneal,* Math. Meth. Appl. Sci. 46(2) (2023) 1511–1527.

[2] Alshammari, A.O., Ahmad, I., Jan, R. and Idris, S.A. *Fractional-calculus analysis of the dynamics of CD4$^+$ T cells and human immunodeficiency viruses*, Eur. Phys. J. Spec. Top. 234(8) (2025) 1991–2003. https://doi.org/10.1140/epjs/s11734-024-01192-5

[3] Amin, R., YÜZBAŞI, Ş. and Nazir, S. *Efficient numerical scheme for the solution of HIV infection CD4$^+$ T-cells using Haar wavelet technique*, Comput. Model. Eng. Sci. 131(2)

(2022) 639–653. https://doi.org/10.32604/cmes.2022.019154.

[4] Arafa A.A.M., Rida S.Z., Khalil M., *Fractional modeling dynamics of HIV and $CD4^+$ T-cells during primary infection*, Nonlinear Biomed. Phys. 6 (2012) 1–7.

[5] Arshad, S., Baleanu, D., Bu, W. and Tang, Y., *Effects of HIV infection on $CD4^+$ T-cell population based on a fractional-order model*, Adv. Differ. Equ. 2017 (2017) 92. https://doi.org/10.1186/s13662-017-1143-0.

[6] Bajaria, S.H., Webb, G., Cloyd, M. and Kirschner, D. *Dynamics of naive and memory CD4+ T lymphocytes in HIV-1 disease progression*, J. Acquir. Immune Defic. Syndr. 30(1) (2002) 41–58.

[7] Baleanu, D., Diethelm, K., Scalas, E. and Trujillo J.J., *Fractional Calculus Models and Numerical Methods*, Series on Complexity, Nonlinearity and Chaos, World Scientific, 2012. https://doi.org/10.1142/8180.

[8] Hasani-Lichae, B., Biazar, J. and Ayati, Z., *The fractional differential model of HIV-1 infection of $CD4^+$ T-cells with description of the effect of antiviral drug treatment*, Comput. Math. Methods Med. 201 (1) (2019) 4059549. https://doi.org/10.1155/2019/4059549.

[9] Culshaw, R.V. and Ruan, S. *A delay-differential equation model of HIV infection of $CD4^+$ T-cells*, Math. Biosci. 165 (2000) 27–39.

[10] Dinga, Y. and Yea, H., *A fractional-order differential equation model of HIV infection of $CD4^+$ T-cells*, Math. Comput. Model. 50 (2009) 386–392.

[11] Diethelm, K. , *The analysis of fractional differential equations*, Springer, Berlin, 2010.

[12] Floater, M.S. and Hormann, K., *Barycentric rational interpolation with no poles and high rates of approximation*, J. Numer. Math. 107 (2) (2007) 315–331.

[13] Fuda, C., *Numerical stability of barycentric interpolation,Doctoral Dissertation submitted to the Faculty of Informatics of the Università della Svizzera italiana*, Doctoral Dissertation submitted to the Faculty of Informatics of the Università della Svizzera italiana, 2024.

[14] Galperin, E.A., Kansa, E.J., Makroglou, A. and Nelson, S.A., *Variable transformations in the numerical solution of second kind Volterra integral equations with continuous and weakly singular kernels; extensions to Fredholm integral equations*, J. Comput. Appl. Math. 115 (1) (2000) 193–211.

[15] Hernandez-Vargas, E.A. and Middleton, R.H. *Modeling the three stages in HIV infection,* J. Theor. Biol. 7(320) (2013)33–40. doi:10.1016/J.JTBI.2012.11.028.

[16] Hilfer, R. (Ed.), *Applications of fractional calculus in physics*. World Scientific, Singapore, 2000.

[17] Katani, R. and McKee, S., *A product integration method for nonlinear second kind Volterra integral equations with a weakly singular kernel (with application to fractional differential equations)*, Appl. Math. Lett. 163 (2025) 109403.

[18] Katani, R. and Shahmorad, S., *A block by block method for solving system of Volterra integral equations with continuous and Abel kernels*, Math. Model. Anal. 20 (6) (2015), 737–753.

[19] Khader, M.M. *The modeling dynamics of HIV and $CD4^+$ T-cells during primary infection in fractional order: numerical simulation*, Mediterr. J. Math. 15(3) (2018) 139. https://doi.org/10.1007/s00009-018-1178-9.

[20] Laurie, D.P., *Periodizing transformations for numerical integration*, J. Comp. Appl. Math. 66 (1-2)(1983) 337–344.

[21] Li, M. and Huang, C. *The linear barycentric rational quadrature method for auto-convolution Volterra integral equations*. J. Sci. Comput. 78 (2019) 549–564. https://doi.org/10.1007/s10915-018-0779-6.

[22] Liu, H., Ma, Y., Li, H. and Zhang, W., *Combination of discrete technique on graded meshes with barycentric rational interpolation for solving a class of time-dependent partial integro-differential equations with weakly singular kernels*, Comput. Math. Appl. 141 (2023) 159–169, https://doi.org/10.1016/j.camwa.2023.04.018.

[23] Ma, J., *A class of reducible quadrature rules for the second-kind Volterra integral equations using barycentric rational interpolation*, J. Comput. Appl. Math. 445 (2024) 115803. https://doi.org/10.1016/j.cam.2024.115803.

[24] McKee, S., Tang, T. and Diogo, T., *An Euler-type method for two-dimensional Volterra integral equations of the first kind*. IMA J. Numer. Anal. 20(3) (2000) 423–440.

[25] O'Regan D., Agarwal R.P. and Perera K. ,*Nonlinear integral equations singular in the dependent variable*, Appl. Math. Lett. 20 (2007) 1137-1141.

[26] Parand, K., Kalantari, Z., Delkhosh, M., *Quasilinearization-Lagrangian method to solve the HIV infection model of $CD4^+$ T cells*, SeMA 75 (2018) 271–283. https://doi.org/10.1007/s40324-017-0133-1

[27] Perelson, A.S., Kirschner, D.E. and Boer, R. De, *Dynamics of HIV infection of CD4C T-cells*, Math. Biosci. 114 (1993) 81–125.

[28] Podlubny, I., *Fractional differential equations: An introduction to fractional derivatives, fractional differential equations, to methods of their solution and some of their applications*, Elsevier, 1998.

[29] Salah, E.Y., Sontakke, B., Abdo, M.S., Shatanawi, W., Abodayeh, K., Albalwi, M.D. and Kamrujjaman, Md., *Conformable fractional-order modeling and analysis of HIV/AIDS transmission dynamics*, Int. J. Differ. Equ. 2024(1) (2024) 1958622.

[30] Sokhanvar, E. and Askari Hemmat, A., *Numerical solution of a fractional model for HIV infection of $CD4^+$ T cells via Legendre multiwavelet functions*, Int. J. Bioautomation 24 (4) (2020) 359–370. doi:10.7546/ijba.2020.24.4.000634.

[31] Yildirim, G. and Yüzbasi, S.,*Numerical solutions of SIRD model of Covid-19 by utilizing Pell-Lucascollocation method*, Turk. J. Math. 48 (6) (2024) 1156–1182.https://doi.org/10.55730/1300-0098.3567

[32] Yüzbasi, S., *A numerical approach to solve the model for HIV infection of $CD4^+$ T cells*, Appl. Math. Model. 36 (2012) 5876–5890.

[33] Yüzbasi, S. and Izadi, M., *Bessel-quasilinearization technique to solve the fractional-order HIV-1 infection of $CD4^+$ T-cells considering the impact of antiviral drug treatment*, Appl. Math. Comput. 431 (2022) 127319. https://doi.org/10.1016/j.amc.2022.127319.

[34] Yüzbasi, S. and Karacayir, M., *An exponential Galerkin method for solutions of HIV infection model of $CD4^+$ T-cells* Comput. Biol. Chem. 67(2017)205–212. DOI10.1016/j.compbiolchem.2016.12.006

[35] Zhao, Z. and Huang, C. *Collocation methods based on barycentric rational interpolation for Volterra integro-differential equations with weakly singular kernels*, Math. Methods Appl. Sci. 48 (2023) 8007–8023. https://doi.org/10.1002/mma.9468.